10 January 2015

TO: FRAPPE data-processing file
FROM: Al Cooper
SUBJECT: Some suggestions re FRAPPE processing for wind and pressure

This memo discusses some studies of the wind measurements for FRAPPE and the related corrections to pressure based on the earlier calibration via LAMS. This version of the memo, V3, pertains to using QCFR/PSFRD as the primary sensors for calculating TASF/TASX and hence for calculating wind. This change was made, from QCF/PSFD, because the latter did not produce wind measurements that were satisfactory in reverse-heading or circle maneuvers and also, in the case of QCF, was inconsistent with other projects in its relationship to QC_A. QCFR/PSFRD appeared to be much better in both those regards. Note, however, that because of this change the sensitivity coefficients describing angle-of-attack and sideslip use QCFR in the denominator of the pressure ratio, so calibration coefficients are slightly different and should not be used for other projects where QCF/PSFD are primary.

1 Calibration of the angle-of-attack

The speed run from 15:50:00 to 15:55:00 on FRAPPE flight 4 provides good data for determining the angle-of-attack sensitivity coefficients. The equation used for the fit is

$$\alpha_{ref} = \theta - \frac{w_p}{V} = b_0 + b_1 \frac{\Delta p_\alpha}{q} \tag{1}$$

where θ =PITCH, w_p =GGVSPD, V =TASX, Δp_α =ADIFR, and q =QCFR. The choice for representing q is based on QCFR being more reliable than QCR and not requiring prior pressure-defect correction as does PSXC (the use of which introduces circularity in the calculation because the pressure correction itself depends on angle of attack. The left side of (1) is equal to the angle of attack if the vertical wind is zero, so the use of this result depends on the calibration maneuver being flown in air without vertical motion.

The details of the fit results are listed below:

```
## lm(formula = AOAREF ~ AQR, data = DataV)
## [1] "Coefficients:"
##              Estimate Std. Error  t value Pr(>|t|)
## (Intercept)  4.859618 0.01453493 334.3408        0
## AQR         14.141572 0.05896064 239.8477        0
## [1] "Residual standard error: 0.113, dof=299"
## [1] "R-squared 0.995"
```

The standard error for the fitted values is $0.113°$ so this is a very good fit, with correlation coefficient of about 0.997. If instead VSPD is used for the vertical-speed variable, the standard error is $0.116°$, only slightly worse, but the coefficients change enough that using the higher-quality GPS
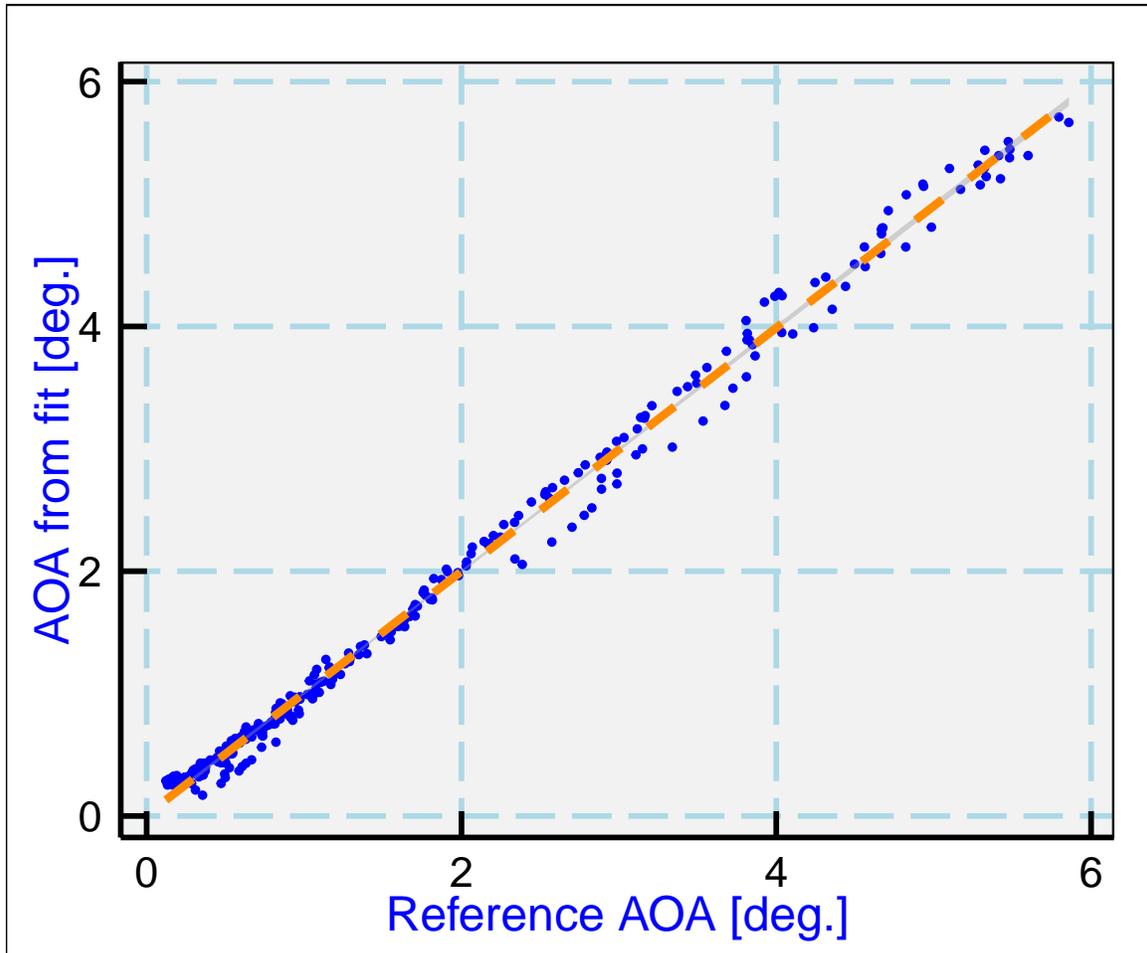
Figure 1: *Fit AOA vs reference AOA (α_{ref}) from Eq. 1. The orange dashed line shows the fit, for which details and coefficients are shown in the text.*

measurement seems preferable. These results are also significantly different from those previously used, but the radome has been changed on the C-130 so that may explain the change in sensitivity coefficients.

2 Corrections to ambient and dynamic pressure

A correction procedure was developed previously for correcting both dynamic and ambient pressure measurements using flights on which the laser air motion sensor (LAMS) was operating. These are described in this paper.[1] However, two problems have arisen in applying those results to the C-130 in FRAPPE. First, the radome on the C-130 was changed and this led to apparent changes in the sensitivity coefficients for measurement of angle of attack, as discussed in the previous section. Because the pressure corrections in that paper were formulated in terms of Δp_α=ADIFR and q_r =QCR, the parameterized fit from that paper no longer applies to the new radome. Second, because the radome dynamic pressure QCR encounters problems with icing or frozen lines more often than the measurement QCF from a pitot tube, the latter is a better choice for representing angle-of-attack and is used in the preceding section to find coefficients for calculating angle of attack. The formula for correcting the pressures therefore needs to be corrected to use angle of attack, to make the correction general and not specific to one radome, and the translation from the previous formulation needs to account for the change in underlying variable QCF instead of QCR.

The correction from the paper referenced above was:

$$\frac{\Delta p}{p} = b'_{0-} + b'_1 \frac{\Delta p_\alpha}{\Delta q_r} + b'_2 M \tag{2}$$

where Δp is the correction to be applied to pressure and M is the Mach number. The Mach number used in the fit was that determined from the uncorrected measurements of ambient and dynamic pressure, which on the C-130 were PSFD and QCF. The coefficients determined by fitting (2) to the corrections determined using LAMS were $\{b'\}$ = {0.00152, 0.0205, 0.0149}. In the document on Processing Algorithms, this formula was transformed to a dependence on angle of attack rather than on the pressures from the radome, leading to this representation for the pressure correction term:

$$\frac{\Delta p}{p} = b_0^* + b_1^* \alpha + b_2^* M \tag{3}$$

where α is the angle of attack. The coefficients are then $\{b^*\}$ = {-0.00637, 0.001366, 0.0149} for PSFD and {-0.00754, 0.000497, 0.0368} for PSFRD. The same corrections apply with reversed sign to QCF and QCFR, respectively. With the new angle of attack determined as in Sect. 1, these results should remain valid for the new radome and so should be applicable to FRAPPE.

---

[1]Atmos. Meas. Tech., 7, 3215-3231, 2014

3 Sideslip

3.1 Sensitivity coefficient

Calibration of the sideslip angle is more difficult, both because the equations are more complicated and because the maneuver is very hard to fly. Ideally, the sideslip maneuver should only change yaw angle and heading without change in roll, altitude, or angle-of-attack, but that is impossible. These maneuvers were flown with primary attention to roll and altitude.

For yaw maneuvers, the calibration is based on the expectation that the horizontal wind remains constant. The first-order equations for the east and north components of the wind, u and v, are:

$$
\begin{aligned}
u &= -U_a \sin(\psi + \beta) + u_p \\
v &= -U_a \cos(\psi + \beta) + v_p
\end{aligned}
\tag{4}
$$

where U_a is the true airspeed, ψ the heading, β the sideslip angle, and u_p and v_p are the eastward and northward ground-speed components of the aircraft. These two equations lead to the following reference formula for β:

$$
\beta^* = -\psi + \arctan\left(\frac{u_p - u}{v_p - v}\right)
\tag{5}
$$

where the second term represents a correction for the change in direction of motion of the aircraft, which is difficult to avoid in the yaw maneuver. The measurements thus provide β^*, an estimate of the sideslip during the yaw maneuvers.

There is, however, a circular component in (5) because it involves the wind components and those require β for their measurement when sideslip changes. To reduce the feedback from this term, the horizontal wind components u and v were low-pass-filtered with periods ranging from 5–30 s and the filtered values were used in (5). The wind should remain steady during the maneuver, so this reduces any false effect of the maneuver on the measurement. This made negligible difference in the fits, and the coefficients obtained were close to those in use for sideslip, so after exploring this the unfiltered values of the wind were used for the following fit.

A relatively simple equation provided a very good fit to the measurements:

$$
\beta^* = e_0 + e_1 \frac{\Delta p_\beta}{q}
\tag{6}
$$

where Δp_β is the pressure difference between horizontally separated pressure ports on the radome and q is the dynamic pressure: $\Delta p_\beta =$BDIFR and $q =$QCFR.

A good set of yaw maneuvers was flown on FRAPPE flight 4, 15:45:10 to 15:46:50, so measurements from that flight period will be used to determine the relationship between the wind-sensing pressure measurements and the change in yaw angle. The measurements from that flight segment gave a good fit to Eq. 6, with the following fit characteristics, as plotted in Fig.~2.
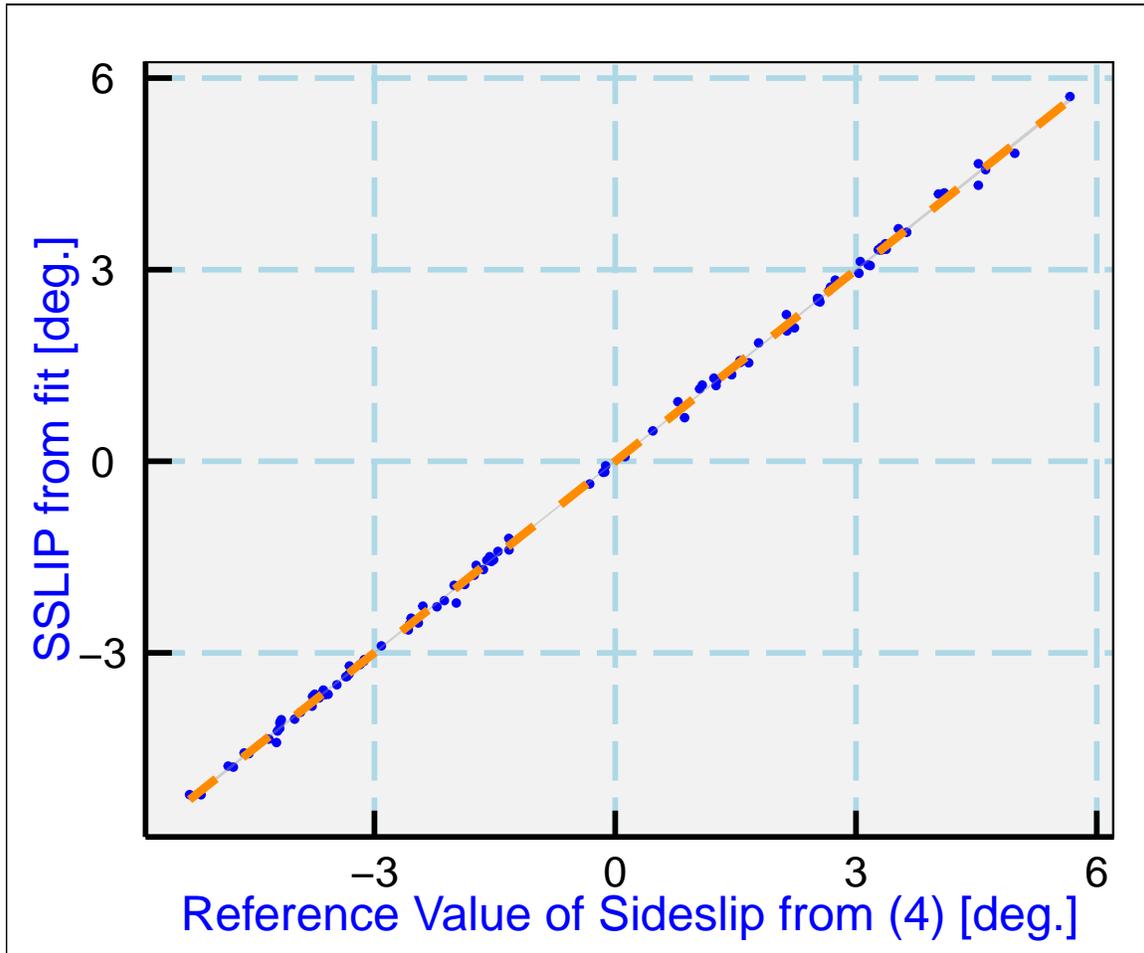
Figure 2: *The sideslip attack determined from the fit, as a function of the reference angle provided by Equation (6), for the data from FRAPPE flight RF04, 154510–154650.*

```
## lm(formula = SSREF ~ BQR, data = DataV)
## [1] "Coefficients:"
##             Estimate  Std. Error  t value      Pr(>|t|)
## (Intercept) 1.379293  0.009515112 144.9582 4.206192e-117
## BQR        13.409806  0.035840276 374.1547 8.706734e-158
## [1] "Residual standard error: 0.082, dof=99"
## [1] "R-squared 0.999"
```

The result from the calibration is also shown in Fig. 2, as the dashed orange line. The square of the correlation was exceptionally high, 0.9993, the residual standard error was 0.08°, and the best-fit coefficients were $\{e_0, e_1\} = \{1.3793, 13.4098\}$. For comparison, the standard values from the calibration of the previous radome were $\{-0.012, 12.21\}$, so the sideslip calibration is significantly different, especially in regard to the constant or offset term, from the old calibration. However, the offset (or first term in the fitted equation) is dependent on the heading being accurate, and the

heading has errors that are different for each flight and during flights. It is therefore useful to check the first coefficient in other ways, either by circle or reverse-heading maneuvers, so this coefficient will be adjusted based on the additional study of such maneuvers that follows.

3.2   Sideslip and heading offsets

Reverse-heading maneuvers

A reverse-heading maneuver was flown on FRAPPE flight RF04, 160000–160245 and 160615–160815. For such a maneuver, if the wind remains constant, the expectation is that the longitudinal and lateral components of the wind each should reverse sign between the two legs. These components are, approximately,

$$v_x = v_g \cos(\xi - \psi) - v_t \tag{7}$$

$$v_y = v_g \sin(\xi - \psi) - v_t \sin\beta \tag{8}$$

where v_g is the ground speed, v_t the true airspeed, ξ the ground-track angle, ψ the heading, and β the sideslip angle.

These components are plotted in Fig. 3, with the primary measurements considered to be PSFRD and QCFR for the calculation of true airspeed and wind as well as for the determination of sensitivity coefficients. The top panel shows that, for the longitudinal component, the reverse-course measurements change from 1.89 to -2.70, so the indicated error is about 0.4 m/s. This is reasonable in comparison to the estimated 0.3 m/s uncertainty in true airspeed, as found from the original LAMS-based PCOR study and as verified in that study by a series of reverse-heading maneuvers. The lateral measurements, shown in the middle panel, also were satisfactory: The values for the two legs were -2.66 and 3.29 indicating a lateral error of about 0.3 m/s. This calculation used the sensitivity coefficients as determined above (with first coefficient for the sideslip calibration 1.3793), but the agreement between the two legs is even better, indicating an error of <0.1 m/s, if the offset is changed to 1.40°. The latter result is shown in the bottom panel of Fig. 3.

When the longitudinal wind was calculated instead from QCF and PSFD, the disagreement in this reverse-heading maneuver was significantly larger, about 2.4 m/s, indicating an error in true airspeed of about 1.2 m/s. A reason for this disagreement has not been found, but comparison of QCF to QC_A shows that this has changed from earlier projects although the similar relationship of QCFR to QC_A has stayed consistent. This suggests a problem with the calibration of QCF, but examination of the calibration records does not indicate any problem. Nevertheless, it appears preferable to use QCFR and PSFRD as primary sensors for FRAPPE.

The conditions were not ideal during this maneuver, however, with important variability along each of the legs as shown in Fig. 3 and with some mis-alignment of the two legs, so it is worthwhile to consider other maneuvers. Another reverse-heading maneuver was flown on flight 9, with reverse legs 19:31:00–19:34:00 and 19:36:10–19:39:10. The sideslip offset determined from this maneuver is slightly larger than that from the Flight-4 maneuver, 1.50° instead of 1.40°, but as
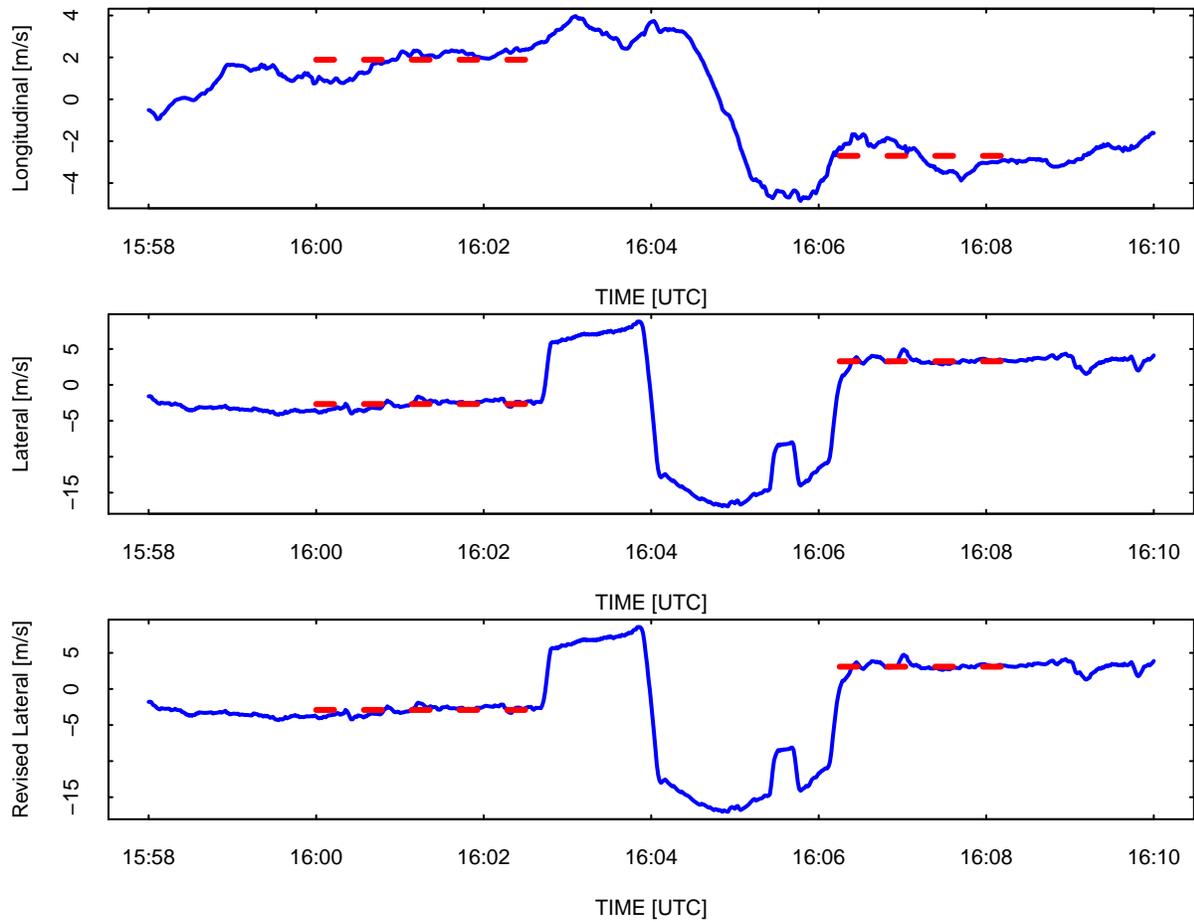
Figure 3: *Wind components measured during the reverse-heading maneuver of FRAPPE flight RF04, 1558–1610. The red dashed lines indicate the straight legs before and after the turn to reverse course and show the mean values averaged over those segments. The top panel shows the longitudinal wind component, the middle panel the lateral wind component as originally processed, and the bottom panel the lateral wind with the new calibration but adjusted to eliminate the offset.*
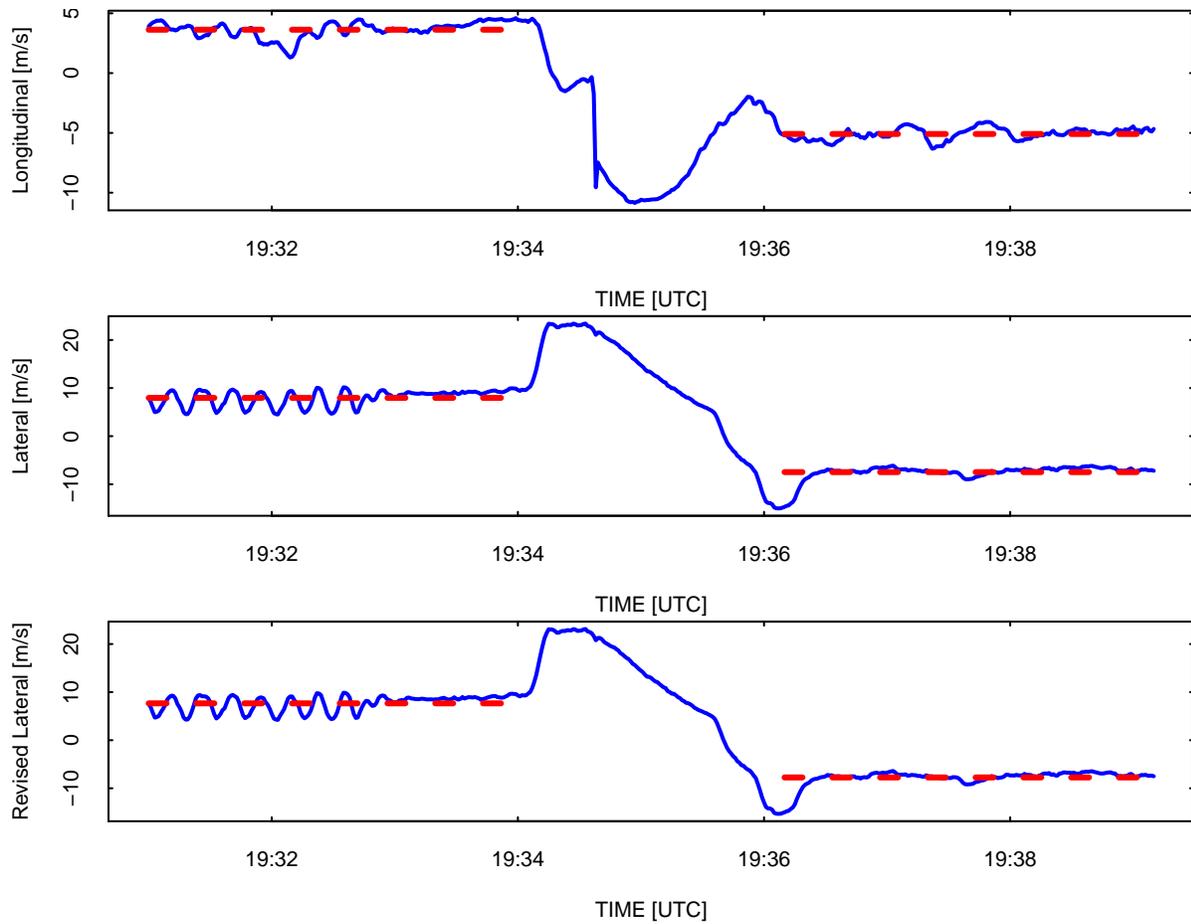
Figure 4: *Wind components measured during the reverse-heading maneuver of FRAPPE flight 9, 193100–193910. The red dashed lines indicate the straight legs before and after the turn to reverse course and show the mean values averaged over those segments. The top panel shows the longitudinal wind component, the middle panel the lateral wind component as originally processed, and the bottom panel the lateral wind with the new calibration but adjusted to eliminate the offset.*
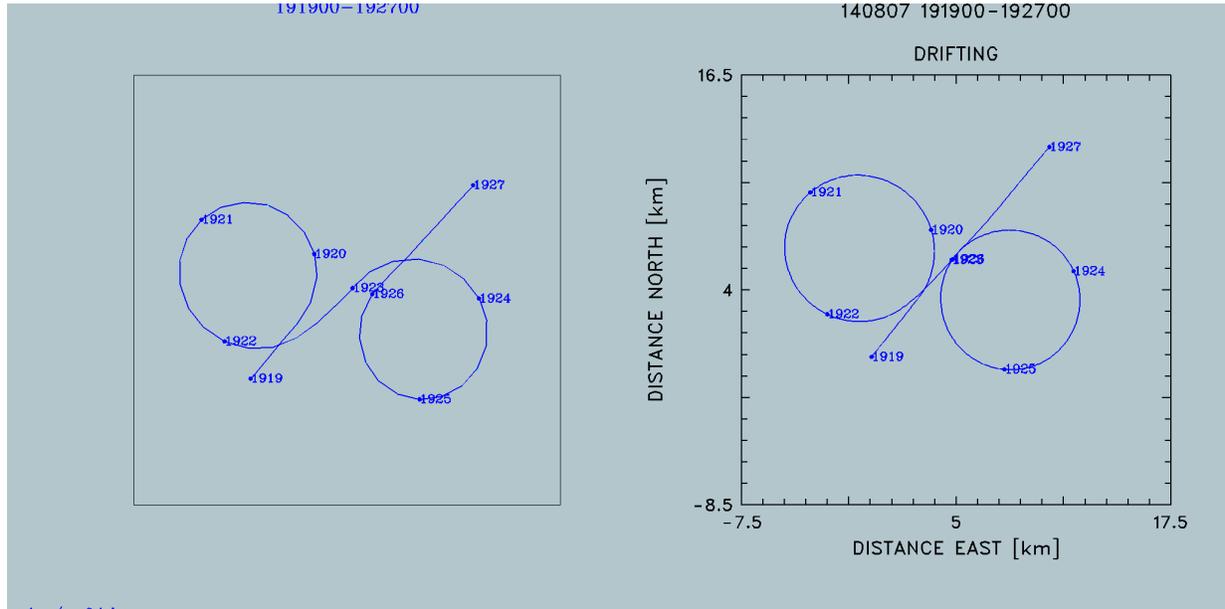
Figure 5: *Example of circle flight pattern, FRAPPE flight 9, 19:19–19:27 UTC. Left side: normal flight track; right side, flight track plotted in a reference frame drifting with the horizontal wind.*

shown in Fig. 4 the conditions were steadier for this case. A remaining source of variability in the sideslip offset determined in this way is error in heading, because it is not possible to separate an offset in sideslip from an offset in heading using reverse-heading maneuvers. Because the heading standard uncertainty is $0.05°$, uncertainty at this level also characterizes the offset in sideslip. This offset will be used for preliminary calculations in the next section, where a further refinement in the sideslip offset can be made.

Circle maneuvers

Another way to determine the offset in sideslip is via circle maneuvers, in which one or more circles are flown at steady bank angle turning one direction and then one or more additional circles are flown in the opposite direction. The measured wind should remain constant around such circles, so any variations can be used to isolate offsets in true airspeed (affecting the measurement of the longitudinal component of the wind) and offsets in sideslip or heading (affecting the measurement of the lateral component). Two such circles were flown from 19:19–19:27 on flight 9, as shown in Fig. 5.

If the wind remains steady around the turns, analyses of the measurements can lead to these results:

1. Wind can be determined from the GPS-measured ground speeds and the heading, with no other reference to the normal wind measurements.

2. Measurement of a possible bias in the true-airspeed measurement TASX: If present, the measured windspeed will change from upwind to downwind direction.

3. Determining biases in heading and sideslip: If present, the measured windspeed will change from crosswind-right to crosswind-left positions.

4. An offset in sideslip can be separated from an offset in heading by checking for the expected sign reversal in sideslip between left-turn and right-turn circles.

5. Departures from constant wind can be used to determine possible time shifts, especially by comparing results from left-turn and right-turn circles.

Each of these will be explored in this section. To get accurate circle patterns, it is important that the wind be relatively steady and non-turbulent and that the roll angle be maintained constant. For this flight segment, the left-turn circles had a roll angle of -26.35 ± 0.18 and the right-turn circles had roll angle 27.81 ± 0.24, while the mean true airspeed for these circles was 142.9 ± 1.8. The steadiness of these measurements indicates that this maneuver was flown with good precision and reasonably symmetrically, although the difference in roll is larger than is characteristic of similar maneuvers with the GV and may indicate some trim adjustment. The mean roll angles are within $1.5°$ and are quite steady for each turn direction, so it will be a reasonable approximation to assume that these patterns are circular.

Because the circles are flown with turn rates of about $1.5°/s$, small errors in the timing of measurements entering the wind calculation can lead to significant errors. The primary comparison used here is to the ground-speed as provided by GPS, so the timing of that signal relative to the corresponding IRU measurements is especially critical for this analysis. As processed, the data file (FRAPPErf09R.nc) used offsets of -2000 ms for GGVEW and GGVNS along with an offset of -80 ms for the IRU measurements including VEW and VNS. High-rate (25 Hz) measurements were used to study the time shifts, in two ways. First, the standard error between GGVNS and VNS, or between GGVEW and VEW, was minimized by shifting GGVNS or GGVEW in time; both comparisons gave minimum RMS errors (of about 0.1 m/s) for a time shift of +11 25-Hz samples, or 440 ms. Second, the heading shift discussed in the next section was used as a test of this result. Without shift in timing, the left-turn circle indicated a heading error of about $+1°$ and the right-turn circle about $-1°$; after timing adjustment of GGVEW/GGVNS by 440 ms, the respective errors were $-0.1°$ and $-0.2°$ for the left-turn and right-turn circles. This confirmed that the dominant contribution to the error in heading was from the time-lag in GGVEW/GGVNS, which would be expected to produce opposite errors for left-turn and right-turn circles.

The indicated shift was 11 samples forward in time; i.e., GGVEW[12] was replaced by GGVEW[1]. In processing, the assumed lag was -2000 ms (GGVEW[1] replaced by GGVEW[101]). This suggests that the time lag of -2000 ms should be replaced by a lag of -1560 ms, if the lag for VEW/VNS is kept at 80 ms. A similar study of the lag applicable to the NOVATEL-GPS measurements GGVNS_NVTL/GGVEW_NVTL indicated that the time shift was +120 ms, placing these measurements 200 ms ahead of the IRU measurements. This relatively small shift probably should be ignored in processing and the lag kept at zero to avoid the awkwardness of positive lag values.

Finding the wind from GPS only   If it is assumed that $\bar{u}_x$, $\bar{u}_y$, TAS, and $\delta\psi$ (the two components of the horizontal wind, the true airspeed, and an assumed error in heading) are constant, then the

expected ground-speed components will be:

$$v_x = \bar{u}_x + TAS\sin(\psi + \delta\psi) \tag{9}$$
$$v_y = \bar{u}_y + TAS\cos(\psi + \delta\psi)$$

where ψ is the heading. The error between these expressions for the ground speed and the measured ground-speed components g_x and g_y then can be minimized to find the four constant parameters in (9) using this expression as a measure of the error:

$$\chi^2 = \sum((g_x - v_x)^2 + (g_y - v_y)^2) \tag{10}$$

The resulting best-fit values, with wind converted to wind direction $\bar{v}_d$ and wind speed $\bar{v}_s$, are shown in Table 1 and plotted in Fig. 6.

Repeating this analysis for the left-turn circles and right-turn circles separately reveals a difference in the deduced wind that is about 1.2 m/s, as also listed in Table 1:

	$\bar{v}_d$ [°]	$\bar{v}_s$ [m/s]	TAS [m/s]	$\delta\psi$ [°]	residual error [m/s]
all turns	283.9	6.4	142.5	−0.1	1.5
mean of measurements	290.0	6.4	142.9		
left turns	277.8	5.7	143.2	−0.1	1.2
right turns	287.2	6.9	141.8	−0.2	0.8

Table 1: *The results obtained by minimizing the error measure (10) for the circle maneuver.*

A plausible case can be made for this difference between left-turn and right-turn circles being real. Figure 7 shows the GPS-derived measurements of ground speed. The amplitude of the variation around the circle is smaller for the left-turn circles vs. the right-turn circles. (The left-turn circle also does not provide nearly as good a fit to the assumption of steady wind as does the right-turn circle.) The difference between maximum and minimum ground speeds is 10.9 m/s for left-turn circles but 14.8 m/s for right-turn circles, indicating a difference in wind speed of −2 m/s between the two turn directions.[2] This difference is determined from the GPS-derived ground-speed measurements only and doesn't involve any other aspect of the wind-measuring systems on the aircraft. Even heading or sideslip can be in significant error without affecting this result for wind speed because the analysis is based only on the maximum vs. minimum values of the ground

---

[2]If circles are fitted to the variations, the result is a difference of −1.7 m/s.

G−EW [blue]; G−NS [green]
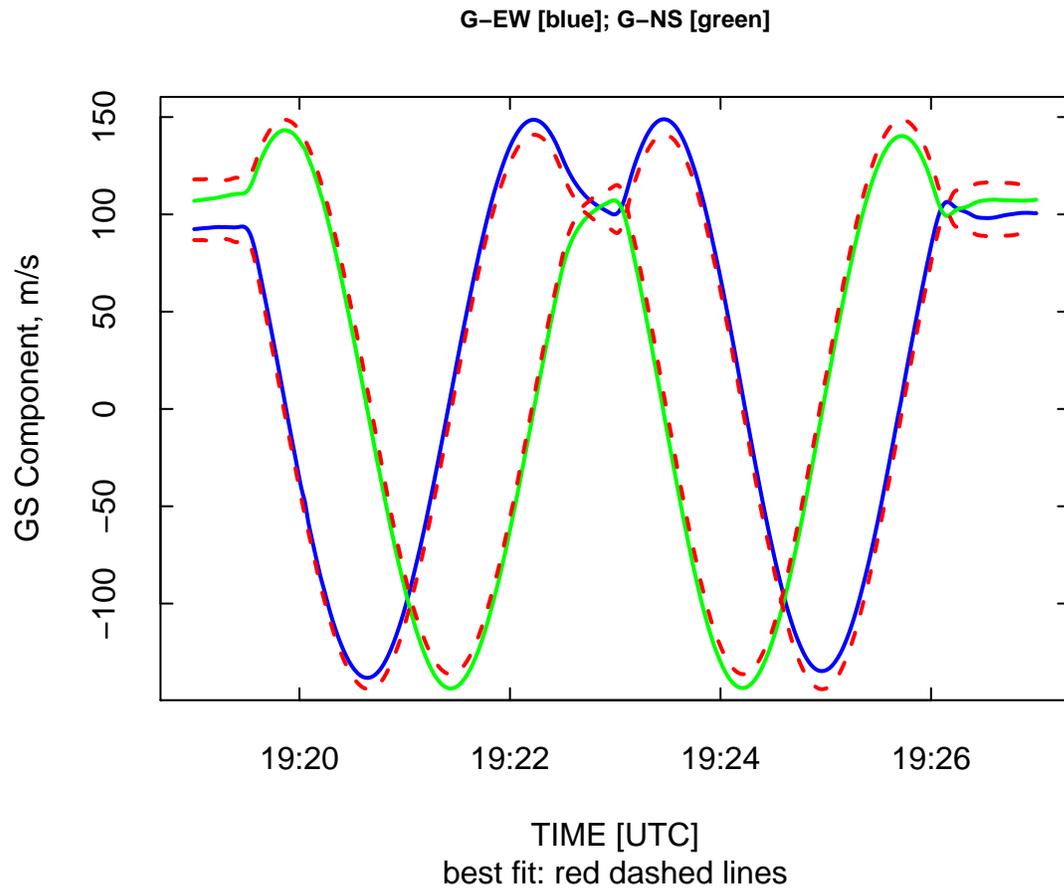
TIME [UTC]
best fit: red dashed lines

Figure 6: *The ground-speed components measured by GPS (blue line, EW; green line, NS) and the corresponding results from the fit (red dashed lines) for the period of the circle maneuver.*
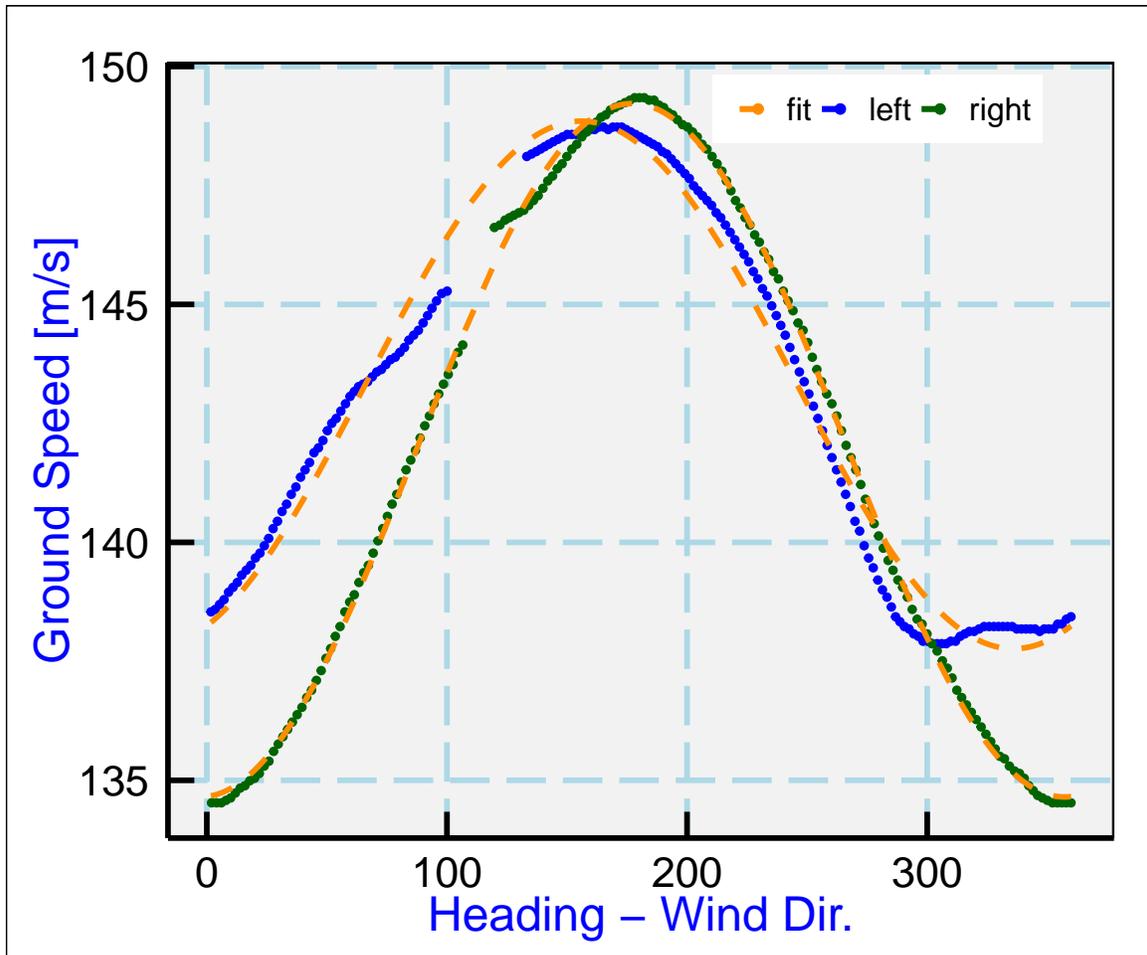
Figure 7: *Ground speed (GGSPD) vs the angle of flight relative to the mean wind direction, for the circle pattern shown in Fig. 5. The dashed orange line represents a fit to a sinusoidal pattern separately for the right-turn and left-turn segments.*

speed. It is expected from instrument specifications that the measurement of ground speed is much less uncertain that this, so the suggested conclusion is that the difference in average wind is real in the regions where the two circles were flown. This difference also contributes to the rather large residual error because the combined fit assumes that a single wind vector characterizes both circles. Figure 7 is evidence that the right-turn circle provides a more consistent result, so that turn direction will be emphasized in the following analysis. That circle indicates that the wind vector is from $287.2°$ at 6.9 m/s and that there is a heading error of $-0.2°$. A -0.2° adjustment in heading, introduced via calibration coefficients, was already made on the basis of a preliminary version of the present study, so this indicates that the heading offset should be reset to zero. However, the angle ψ contains not only any error in heading but also any error in sideslip, so this result will be refined below where those errors are determined separately.

The preceding fit used a constant true airspeed, but it is also possible to fit in the same way for an assumed error in true airspeed, by using $V = V_m + \delta V$ where V_m is the measured value and δV is an assumed error in that measurement. There is some small variation in measured true airspeed during the maneuver, perhaps created by the normal oscillation that results from the flight management system, so this approach may be preferable. However, the resulting best-fit values were very close to those shown in Table 1.

Offsets in TAS and heading An alternate way of determining the offsets in airspeed and heading, which illustrates the value of the circle maneuver for developing these constraints, is to plot the dependence of measured wind speed v_s on the heading. The expected variation is for v_s to change by $2\delta V$ from upwind to downwind flight and by $2V\delta\psi$ from crosswind-right to crosswind-left flight direction (i.e., 90° right of downwind vs. 90° left). The net effect is to produce a variation in v_s given by:

$$v_s = \bar{v}_s + \delta V \cos\gamma + V \delta\psi \sin\gamma \tag{11}$$

where γ is the difference between the heading and the wind direction. Figure 8 illustrates the expected dependence that would result from errors of $\delta V = 1$ m/s and $\delta\psi = 0.3°$. The plot is constructed so that 0° corresponds to downwind flight and the difference between values at 0 and 180°corresponds to $2\delta V$, while the difference from 90 to 270° represents $2V\delta\psi$.

It is then possible to determine δV and $\delta\psi$ by fitting (11) to observations. The measurements will be shown separately for the left-turn circles and the right-turn circles because there is a difference between them. Figures 9 and 10 show the measurements, and the results of the fits are shown in Table 2. The plots do show a sinusoidal pattern as expected from Fig. 8, but there is significant scatter. For the more reliable case shown in Fig. 10, the total standard deviation in measured wind speed is about 0.5 m/s, indicating an uncertainty limit within that range, but the weak sinusoidal pattern also indicates the presence of systematic error. The fit indicates that the error in true airspeed is about 0.2 m/s and the error in heading is about $-0.21°$ after adding the measured sideslip (using first-coefficient 1.5 for sideslip, following the indication from the second reverse-heading maneuver).
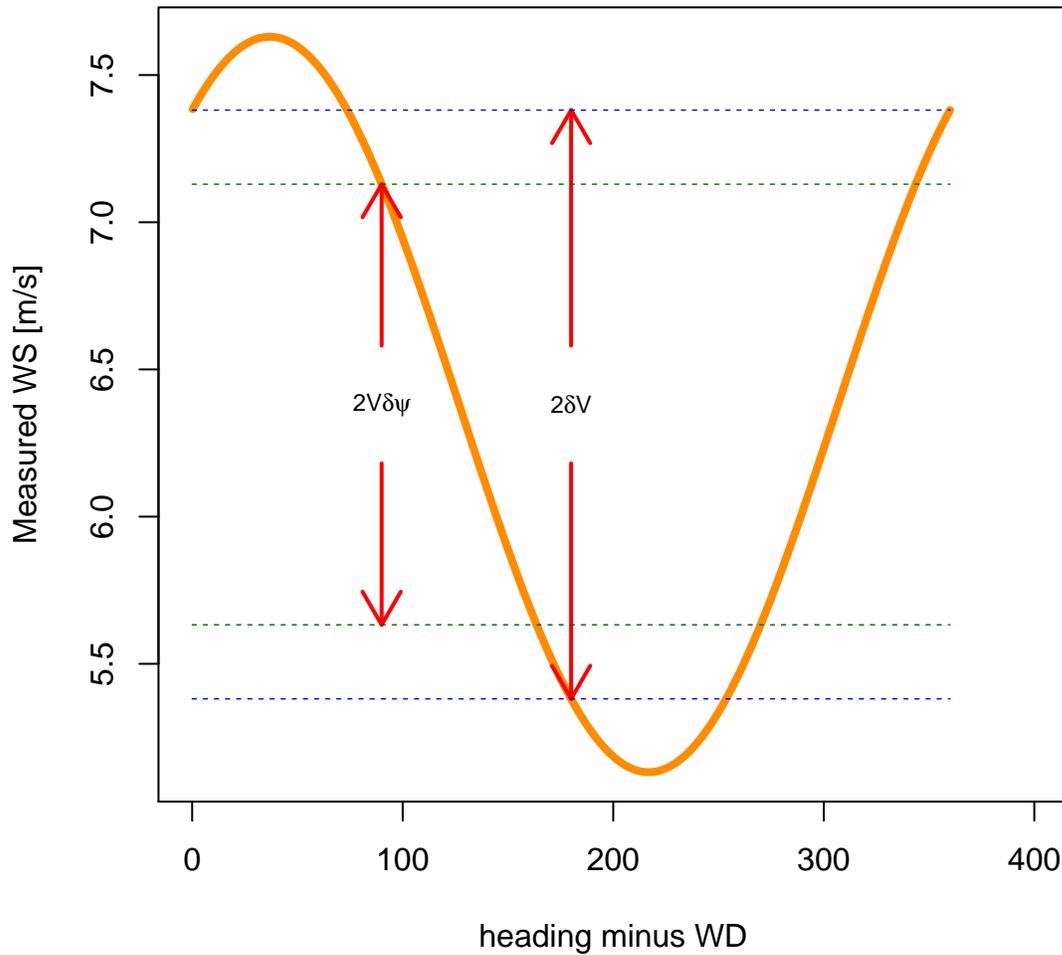
Figure 8: *Predicted dependence of measured wind speed on direction of flight relative to the wind direction, for assumed errors of $\delta V = 1$ m/s and $\delta \psi = 0.3°$.*

	mean wind [m/s]	δV [m/s]	$\delta \psi'$ [°]	residual error [m/s]
left-turn circles	6.4	0.7	-0.07	0.52
right-turn circles	6.3	0.2	-0.21	0.37

Table 2: *Fit results for the left-turn and right-turn circles as fitted by (11). The angle $\delta \psi'$, referred to as the heading error, is actually a combination of heading and sideslip error as given by Eq. 12. See revised values later in Table 3, where the heading error is separated from the sideslip error.*
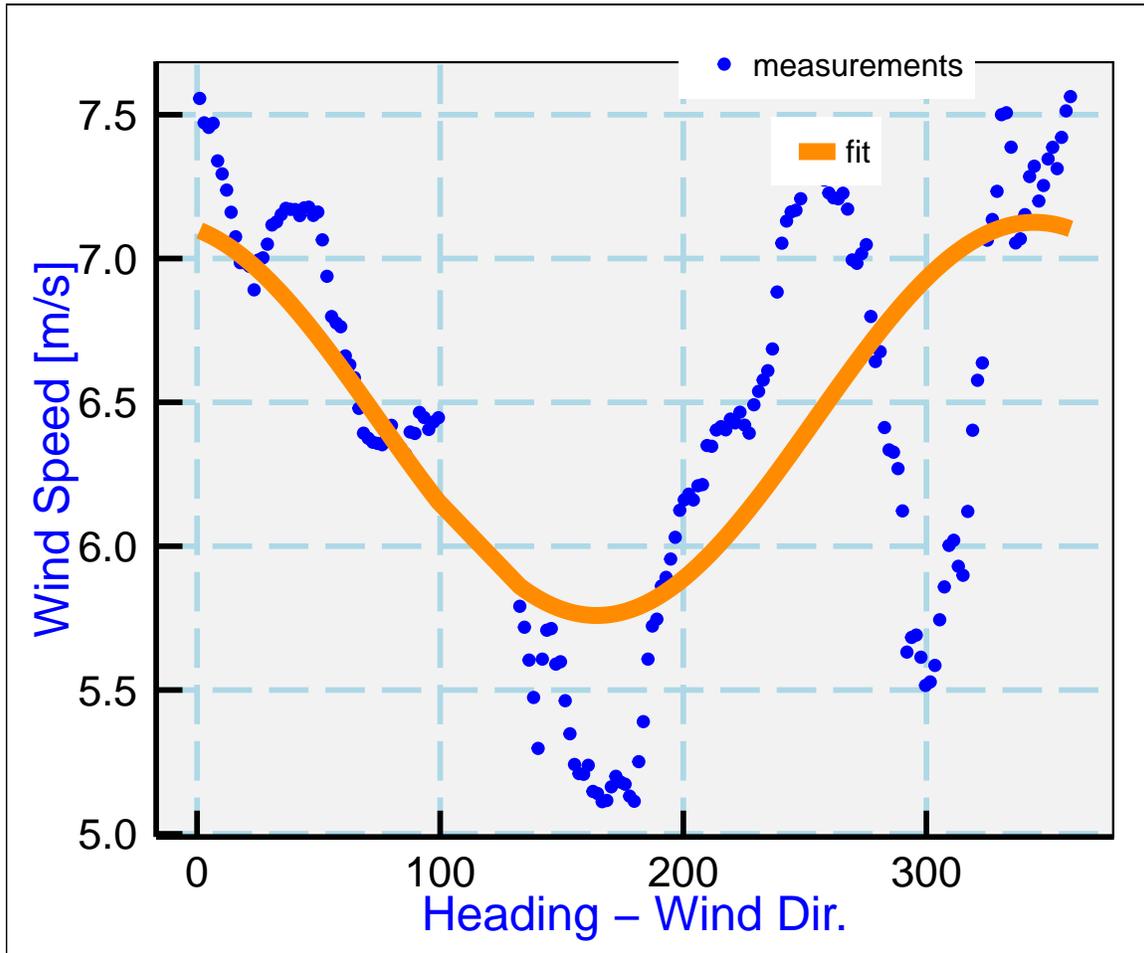
Figure 9: *Measured wind speed from the left-turn circles in the circle pattern shown in Fig. 5, as a function of the difference between the heading and the mean wind direction.*

Sensitivity tests, in which a fixed offset was added first to TASX and then to THDG, showed that adjustments had the expected results: Addition of the negative of the indicated errors resulted in revised estimates near zero. This indicates that, despite the large deviations from the sinusoidal pattern in the wind (as shown in Fig. 10, esp. near the 270° direction), the fit results have the expected dependence on error in the true airspeed or heading.

Offset in Sideslip   In the preceding, the error $\delta\psi$ was discussed as an error in heading, but the error could also be one in sideslip. These errors are difficult to separate and normal reverse-heading maneuvers do not provide a separation. Furthermore, heading errors likely change during a flight because error terms undergo a Schuler oscillation and are also affected by horizontal accelerations such as occur persistently in turns like those in the circle maneuver. The error term determined as in the above tables is $\delta\psi'$ given by
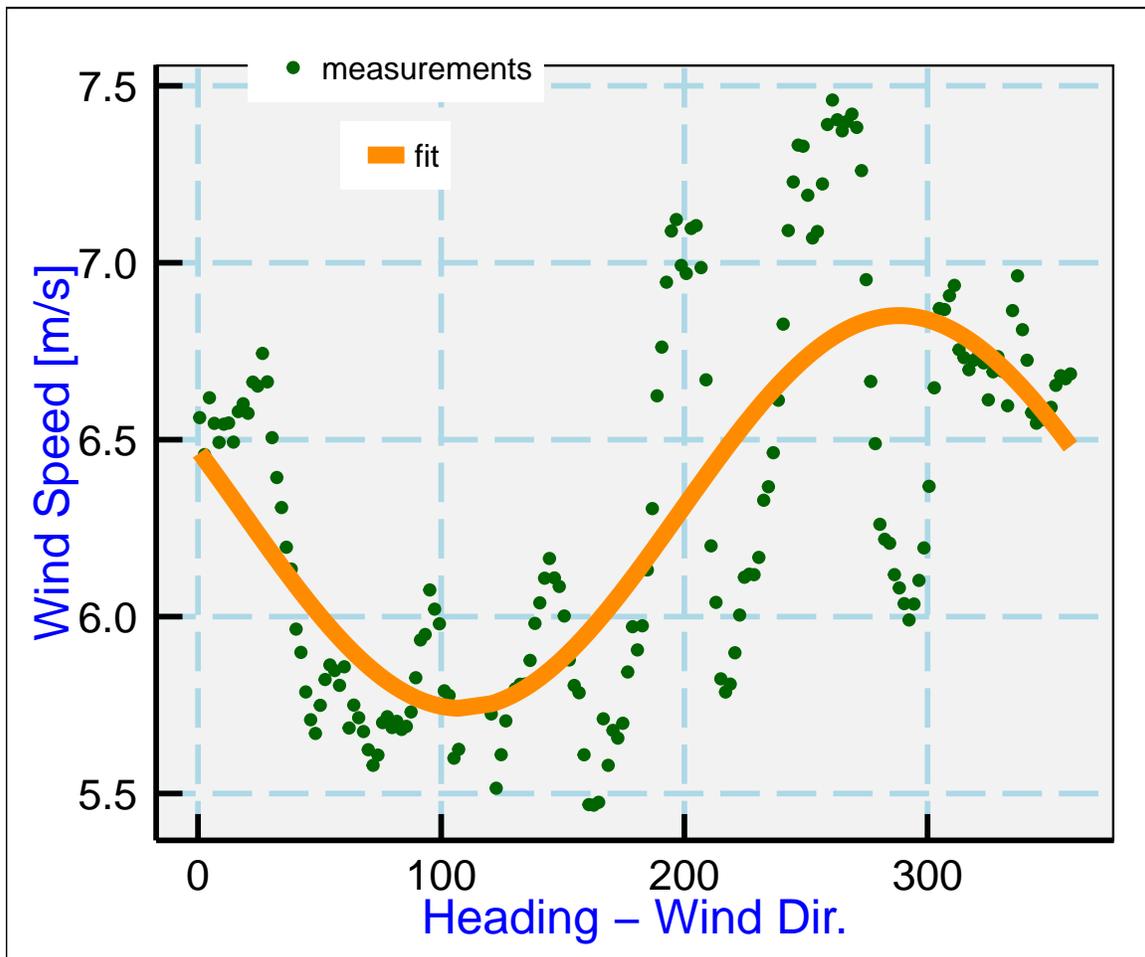
Figure 10: *As for Fig. 9 but for the right-hand circles.*

	mean wind [m/s]	δV [m/s]	$\delta\psi$ [°]	residual error [m/s]
left-turn circles	6.4	0.7	0.02	0.52
right-turn circles	6.3	0.2	-0.11	0.37
combined	6.4	0.4	-0.05	0.5

Table 3: *Fit results for errors in true airspeed V and heading ψ and the residual errors for the fits of Eq. 11 on page 14 to the circles.*

$$\delta\psi' = \delta\psi + \cos\phi\,\delta\beta \tag{12}$$

where ϕ is the roll angle and $\delta\beta$ is the offset in sideslip. The sideslip calibration initially was determined from yaw maneuvers, but those maneuvers also cannot separate an offset in heading from an offset in sideslip so the first coefficient in the calibration, representing the zero offset, is not constrained well by these maneuvers. Because the dependence in (12) is on the cosine of the roll which is an even function, left and right turns are affected in the same way and cannot distinguish the two terms in the equation.

Two approaches could be taken. Because the roll angle changes when circles are flown at different altitudes, results from different-altitude circles could be used to distinguish a sideslip offset from a heading offset. Perhaps a more straightforward test, though, is to compare the sideslip measurement in left vs right turns. In these two cases, some sideslip is introduced as the aircraft configuration remains slightly nose-up during the turn, and that sideslip should reverse sign by symmetry. The lift required to maintain altitude would be the same if the roll angles were opposite, as they nearly are for these maneuvers (1.46° larger for right turns), and the angle of attack is also close to the same, so the expected sign reversal in sideslip can be used to determine the offset in sideslip. The measurements of sideslip are shown in Fig. 11. The red dashed line shows the indicated offset (-0.11°) that is required if the two turn directions are to have the same magnitude of sideslip. Because 1.5° was already used as the constant coefficient in sideslip calibration, this indicates that the best value of the first calibration coefficient (e_0 in Eq. 6) is 1.61; i.e., the resulting sensitivity coefficients for sideslip should be $\{e_o, e_1\} = \{1.61, 13.41\}$. The estimated standard uncertainty in the first coefficient is about 0.1 on the basis of differences among the various estimates of this coefficient and on the basis of uncertainty in the heading measurement on which some of these calibration methods depend. The uncertainty in the second coefficient, estimated from the standard uncertainty with which the slope could be determined in Fig. 2, is about 0.04,

With this shift applied, the dependence of the wind speed on flight direction for the combined left-turn and right-turn circles is shown in Fig. 12. The best-fit coefficients are as shown in Table 3, where the values for left-turn-only and right-turn-only measurements are repeated and shown with the results from both circles combined.
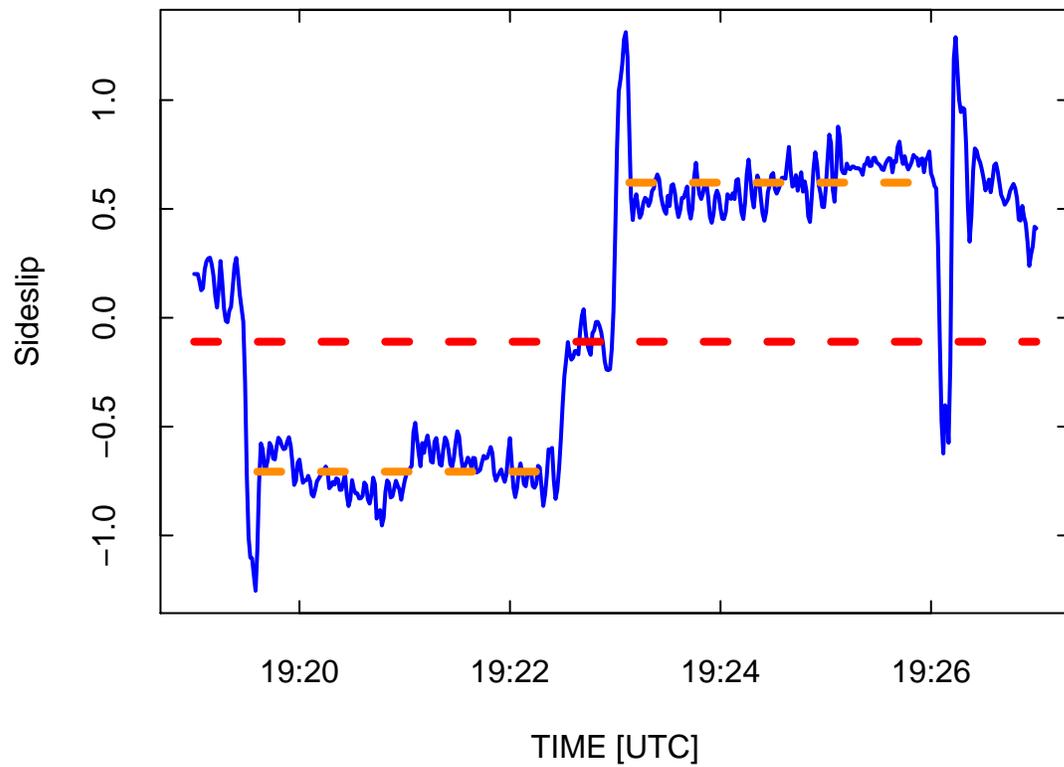
Figure 11: *Measurement of sideslip during the circle maneuver from FRAPPE flight 9, with left-turn circles from 19:19:36 – 19:22:28 UTC, followed by a straight segment and then right-turn circles 19:23:08 – 19:26:02 UTC.*
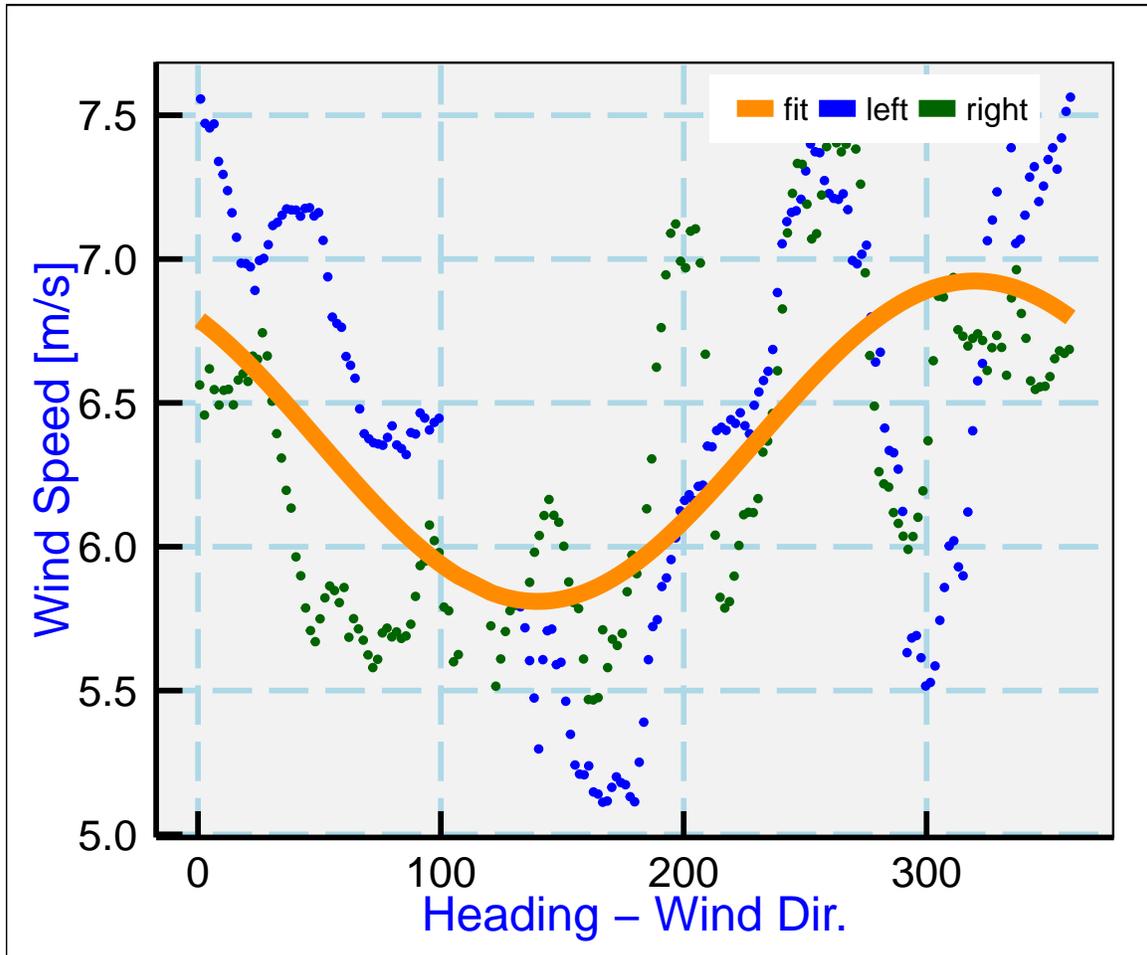
Figure 12: *Wind speed as a function of heading relative to the wind direction, with a fit to the combined data set shown.*

angle	c_0	c_1
AKRD	4.860	14.142
SSRD	1.610	13.410

Table 4: *Recommended sensitivity coefficients for the C-130 in FRAPPE.*

4 Recommendations, angle of attack, sideslip, heading, and true airspeed

4.1 Sensitivity coefficients:

The coefficients in Table 4 include all adjustments discussed in this memo and should be the best to use for FRAPPE, provided that the dynamic pressure measurement QCFR is used in the equations for calculating angle-of-attack and sideslip from ADIFR and BDIFR. The coefficients are dependent on the accuracy of the attitude angles provided by the IRU and will be changed in cases where the pitch or heading aligns differently or otherwise develops errors different from those at the time these coefficients were determined. Both angles have uncertainty of about $0.05°$, so that contributes to the uncertainty in results from these fits.

4.2 Pressure corrections for the static defect

With the angle of attack determined as in Table 4, the formula for C-130 pressure corrections that was previously determined should remain valid. The formulas for PSFD, QCF, PSFRD, and QCFR are given with Eq. 3 on page 3 of this memo.

4.3 GPS timing

The time shift for variables like GGVEW/GGVNS should be -1540 instead of -2000.

4.4 Corrections to TAS, sideslip, and heading (V, β, ψ) :

No corrections are needed except that for sideslip (already incorporated into the coefficients in Table 4) and perhaps a minor change in the heading offset (below). The results from the circle maneuver analyzed here are summarized in Table 5. The indicated quantities are errors, so correction terms would be the negative of these errors. The right-turn circle maneuver, which appears to be in more steady conditions than the left-turn circle and is therefore the basis for these recommendations, indicates that the airspeed may need adjustment by -0.2 m/s. This is small enough and still

type	true airspeed error δV [m/s]	sideslip error $\delta\beta$ [°][a]	heading error $\delta\psi$ [°]
left-turn	0.7	-0.11	0.02
right-turn	*0.2*	*-0.11*	*-0.11*
combined	0.4	-0.11	-0.05

Table 5: *Angle and airspeed adjustments suggested from the circle maneuver of FRAPPE flight 9, 19:19–19:27 UTC. The highlighted results from the right turn appear to be more reliable than those from the left turn or the combined results because conditions were more uniform around the right-turn circle.*

[a]included in Table 4 above for SSRD

has uncertainty of about 0.2 m/s, because the conditions during this circle maneuver were not as steady as desirable, so it appears preferable to make no further correction to the true airspeed. The heading correction of -0.11 is also quite small, and the analysis was done on a data file where the assumed calibration coefficients for heading were {-0.2, 1.0}, so the indication here is that these calibration coefficients should either be changed to {-0.1, 1.} or {0.,1.}. Because the different ways of determining this heading offset produced answers that varied by about $0.1°$, it may be best to change the heading offset to -0.1 and consider the uncertainty to be about of this magnitude.

– End of Memo –

Reproducibility:

PROJECT:	FRAPPEprocessing
ARCHIVE PACKAGE:	FRAPPEprocessing.zip
CONTAINS:	attachment list below
PROGRAM:	FRAPPEprocessing.Rnw
ORIGINAL DATA:	/scr/raf/cooperw/FRAPPE/rf09R.nc, /scr/raf/cooperw/FRAPPErf04R.nc
NIMBUS CONFIGURATION FILE:	/scr/raf/cooperw/FRAPPERHa (high rate)
ARCHIVED SUBSET DATA:	FRAPPErf09R.Rdata, FRAPPErf04R.Rdata
GIT:	https://github.com/WilliamCooper/FRAPPE.git

Attachments: FRAPPEprocessing.Rnw
                FRAPPEprocessing.pdf
                FRAPPErf04R.Rdata
                FRAPPErf09R.Rdata
                FRAPPERHa
                SessionInfo

Some relevant cal coefficients in netCDF files used:
QCFR:CalibrationCoefficients = -0.300948f, 13.8181f, -0.00388295f ;
ADIFR:CalibrationCoefficients = 0.0265582f, 6.99825f, 0.00506988f ;
BDIFR:CalibrationCoefficients = -0.164478f, 5.16347f, -1.19682e-05f ;
THDG:CalibrationCoefficients = -0.2f, 1.f ;
QCF:CalibrationCoefficients = 1.18249f, 17.2991f, -0.00421515f ;